Theory and Observation of Self-Trapping of Resonance Radiation in Gadolinium Chloride*

U. El-Hanany, G. Rakavy, J. J. Wagschal, and S. Yatsiv
Department of Physics, The Hebrew University, Jerusalem, Israel
(Received 2 October 1964)

Self-trapping of resonance radiation in gadolinium chloride is experimentally and theoretically investigated at 77°K. The dependence of the self-reversed line shapes on crystal thickness is used to distinguish between different elementary line profiles. By comparing the observed dependence of the peak separation on crystal thickness with theory, it is shown that the lines have Lorentzian profile. This indicates that the elementary profile of the lines is determined by lifetime broadening due to relaxation processes. The mean free path and width of the lines are also obtained by this method. A direct observation of the line profile seems to be difficult in the present case. The Boltzmann equation for transport of photons in planar geometry is solved numerically for Lorentzian and Gaussian line profiles. The dependence of line shape on crystal thickness and on direction of observation is calculated. Results of calculations of the amplification of nonresonant lines accompanying the resonance emission, and the lengthening of the period of the fundamental decay mode of the resonance radiation in the crystal, are also presented.

I. INTRODUCTION

THE absorption and fluorescence spectra of gadolinium chloride ($GdCl_3 \cdot 6H_2O$) were extensively investigated.[1] The first excited state $^6P_{7/2}$ lies about 32 000 cm^{-1} above the $^8S_{7/2}$ ground state. Each of these two states is split by the crystalline electric field into four Kramers doublets. The spacing between the $^6P_{7/2}$ sublevels is of the order of 20–30 cm^{-1} and that of the $^8S_{7/2}$ is about 0.2 cm^{-1}. The small splitting of the ground state is due to the absence of orbital angular momentum.

Trivalent gadolinium exhibits strong fluorescence in a number of different compounds. The large energy gap (see Fig. 1) between the $^6P_{7/2}$ metastable excited state and the ground state is favorable for a high quantum yield. At liquid-nitrogen temperature linewidths of the four transitions from the $^6P_{7/2}$ sublevels are of the same order of magnitude, 1 cm^{-1}. This width is large compared with the splitting of the ground state, which may therefore be considered as degenerate.

In the chloride, and in a number of other crystals, there is a well-developed vibronic structure accompanying the parent resonance transition.[2] In absorption spectra the vibronic lines appear mainly at the short wavelength side of the parent electronic transition, whereas in emission they are at the mirror image on the long-wavelength side. The most conspicuous vibronics in the chloride are due to water molecules surrounding the gadolinium ion.

From the very early stages of this study we observed that the intensity of the emission vibronics is temperature-dependent and may vary considerably from sample to sample. For example, in a well-ground crystalline powder the intensity of the 3470 Å water vibronic is only few percent of that of its parent resonance transition. This relative intensity rises to more than 50% in large and polished samples at particular orientations with respect to the incident radiation.

Considering the energy diagram, Fig. 1, it was suspected that the observed intensity variations were due to self-trapping of the resonance radiation. The emitted vibronic is not reabsorbed in the crystal since the excited vibrational state $v(1)$ is not populated at room or lower temperatures. It follows that in each emission-reabsorption cycle of the resonance radiation some of the intensity is transferred to the vibronic lines. The enhancement of the vibronics increases with the thickness of the crystal. Internal reflections on polished surfaces have a similar effect as that of increasing the crystal.

Self-trapping manifests itself in two additional phenomena well known from the case of resonance emission in a gas discharge[3]: (1) self-reversal of the lines; (2) an increase in the luminescence decay time. These two phenomena have actually been observed in the gadolinium chloride crystals. Measurements of the distance between the two peaks of self-reversed lines, as a function of crystal thickness, served to determine the profile of the lines and the mean free path of the resonance radiation.

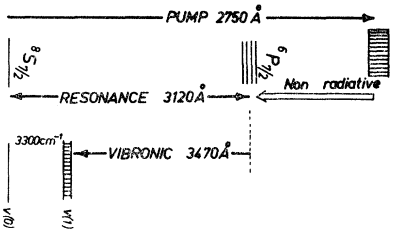

FIG. 1. Schematic energy levels diagram of gadolinium in $GdCl_3 \cdot 6H_2O$.

* Work supported in part by the National Bureau of Standards, Washington, D. C.

[1] G. H. Dieke and L. Leopold, J. Opt. Soc. Am. **47**, 944 (1957).

[2] A. N. Zaidel, G. S. Lazeeva, G. V. Ostrovskaya, and P. P. Yakimova, Bull. Acad. Sci., USSR, Phys. Ser. **26**, 74 (1962); S. Yatsiv, I. Adato, and A. Goren, Phys. Rev. Letters **11**, 108 (1963).

[3] G. H. Dieke and R. D. Cowan. Rev. Mod. Phys. **20**, 418 (1948); A. M. Samson, Opt. i Spectroskopiya **8**, 89 (1960) [English transl.: Soviet Phys.—Opt. Spectry. (USSR) **8**, 43 (1960)]; W. Zwicker, Z. Physik **166**, 148 (1962).

Extensive literature can be found on imprisonment of resonance radiation. A thorough discussion and references to earlier work on this subject are found in the work of Holstein.[4] The Boltzmann transport equation for the excitation state was rigorously formulated by Holstein and approximately solved by variational methods. In particular, he discussed the lengthening of the decay time of trapped radiation. A different approach which is probably more adaptable to experimental observation of the lengthening of decay time was given by Samson.[5]

Self-reversal of resonance radiation was discussed by Dieke and Cowan[6] and by Zwicker.[7] These works were concerned, however, with the absorption of the resonance radiation in the active medium and not with self-trapping.

The present work deals with self-reversal in systems with a high quantum yield and a planar geometry. The exact Boltzmann equation is solved and in this sense the present work is an extension of Holstein's original theory of the effects of self-trapping on line shapes.

II. EXPERIMENTAL PROCEDURES

Crystals of gadolinium chloride were grown by slow evaporation from saturated aqueous solutions. Large

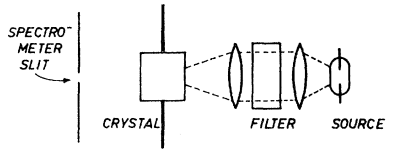

FIG. 2. Experimental arrangement for observing self-reversed resonance lines.

(4 cm) single crystals were easily obtained in a few weeks. These crystals are very hygroscopic and a careful handling with dry-box technique was necessary to prepare samples with uniform cross sections. The transparency of the crystals is sensitive to thermal treatment; it is impaired when the crystal is cooled to liquid-nitrogen temperature, and warmed up, even slowly, to room temperature.

Spectrograms of resonance and vibronic lines were obtained with high resolution (1 cm^{-1}) in a Jarrel-Ash 1.8-m scanning spectrometer of the Ebert-Fastie design. A 500-W Philips high-pressure mercury lamp was used as a source and a 6255B EMI photomultiplier served as a detector. Suitable interference filters were interposed to eliminate redundant orders from the spectrometer. To avoid the warming up of the crystalline sample, under the intense uv radiation, a specially designed cryostat was used. The sample was dipped in the cooling liquid contained in a rectangular quartz cuvette. The cuvette was attached to the internal container of the cryostat.

[4] T. Holstein, Phys. Rev. **72**, 1212 (1947).
[5] A. M. Samson, Ref. 3.
[6] G. H. Dieke and R. D. Cowan, Rev. Mod. Phys. **20**, 418 (1948).
[7] W. Zwicker, Z. Physik **166**, 148 (1962).

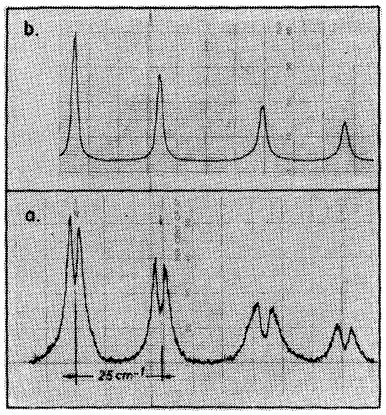

FIG. 3. Resonance fluoresence in $GdCl_3 \cdot 6H_2O$ at 77°K. (a) Shape of lines observed in the forward direction. (b) Shape of the same lines observed in the backward direction.

The uv pumping radiation, around 2750 Å, is strongly absorbed; its mean free path in the crystal is about 10^{-2} cm. Thus, a surface source of resonance radiation is formed at the illuminated side of the crystal. Consequently, the unusual geometry illustrated in Fig. 2 was adopted. The spectrograms of emission lines obtained in this geometrical arrangement revealed strong self-reversal of the four resonance transitions [Fig. 3(a)]. This should be contrasted to the same lines obtained in the usual geometrical arrangement in which the emitted radiation is observed from the side receiving the pumping radiation [illustrated in Fig. 3(b)].

The focusing of the incident pumping-radiation was intentionally varied to check the sensitivity of the self-reversed profile to the geometry of the excitation. For the same purpose, reflectors were attached to the surfaces of the crystal parallel to the incident radiation. The self-reversed profiles were found to be insensitive to these variations. It is stipulated therefore, that edge effects are unimportant and that for the purpose of analysis, the crystal and the illuminated spot can be considered to have infinite cross section.

The spectrometer f number is about 24. Consequently, the angular aperture of radiation which enters the spectrometer is small. This is important since the shape of the self-reversed line depends on the direction of observation.

III. SHAPES OF NARROW LINES IN CRYSTALS

Optical transitions of rare-earth ions in crystals are usually "narrow" in the sense that their width is much smaller than the Debye frequency of the lattice vibrations.[8]

At low temperatures, some of the rare-earth transitions are so sharp and weak that their apparent width is determined by the experimental resolution rather

[8] A. L. Schawlow, *Proceedings of the Third International Conference on Quantum Electronics* (Columbia University Press, New York, 1964), p. 645.

than by the physical mechanisms. Also in the present investigation the slit width was not small enough and the line shapes were modified by the finite band pass. Besides, the resonance lines in gadolinium chloride are never free of broadening due to self-trapping and their "true" profiles could not be observed directly.

Fortunately, as will be shown, self-reversal happens to serve as an indication for the "elementary" line profile. In order to use this indirect method of determining line profiles we have to assume some distinct form for the profile and then check the consistency of this assumption with the measurements. A choice of "reasonable" line profiles falls back on theoretical reasoning.

There has been extensive theoretical research in the past three years on the width and shape of "narrow" lines in crystals.[9,10] Two mechanisms that contribute mostly to linewidths are:

(1) Inhomogeneity of the crystalline field. This is due to random local static strains and the inhomogeneity of the local Stark pattern at different sites in the crystal. Lines produced by this broadening have a Gaussian shape.

(2) Relaxation broadening. The contribution of relaxation to optical widths in crystals has attracted little attention in the past. It has been realized in the last few years[9–12] that this is a major factor determining the width of rare-earth-ion transitions in crystals. The spacing of 10–100 cm^{-1} between close-lying Stark components of such ions is well within the Debye frequency spectrum of lattice vibrations. Effective relaxation involving direct and Raman-type phonon transitions can therefore take place between these levels. The transition probabilities are in the range of 10^8–10^{12} sec^{-1} and can therefore account for the temperature-dependent part of the linewidths.[10] The resulting lifetime broadening in a group of Stark levels has a typical low-temperature behavior which was actually observed.[11] Lifetime broadening contributes a Lorentzian-type profile.

The first mechanism, broadening due to inhomogenities of the crystalline field, is not effective in the case considered in this work. The crystals are grown slowly and at a constant temperature from water solutions, a process which is unlikely to produce thermal strains. In contrast with thermally grown crystals, no variation is observed in the linewidths of samples grown at different rates and temperatures.

It is therefore likely that at liquid-nitrogen temperatures the elementary profile will be Lorentzian.

[9] D. E. McCumber and M. D. Sturge, J. Appl. Phys. 34, 1682 (1962).
[10] W. M. Yen, W. C. Scott, and A. L. Schlawlow, Phys. Rev. 136, A271 (1964).
[11] S. Yatsiv, Physica 28, 521 (1962).
[12] A. Kiel, Phys. Rev. 126, 1292 (1962); Johns Hopkins University Radiation Laboratories Technical Report AF 93,1962 (unpublished).

IV. THE EMISSION AND ABSORPTION OF RESONANT RADIATION

A rough measurement of the mean free path of the pumping and resonance radiations and linewidths and decay rates of the resonance radiation yields the following model for the self trapping in the present case:

The incident pumping radiation is completely absorbed in a very thin layer (10^{-2} cm) at the front surface of the crystal. The excitation decays by fast relaxation to the four sublevels of the $^6P_{7/2}$ state. Between these sublevels there is an intense excitation shuffling due to relaxation mechanisms. Besides, at temperatures of liquid nitrogen or lower, all four sublevels decay predominantly by radiative transitions to the ground state. The radiative decay rate (10^{-2} sec^{-1}) is very low compared with the relaxation transition frequency (10^{10} sec^{-1}). Consequently, the relative population of the $^6P_{7/2}$ sublevels obeys a Boltzmann distribution corresponding to the lattice temperature. The observed intensities of the four lines are proportional to the same Boltzmann factor $[\exp(-\Delta_i/kT)]$ which governs the population of the sublevels. Hence, the sum of squares of transition dipoles between each of the $^6P_{7/2}$ sublevels and the ground-state sublevels is approximately the same. This is also in accord with the observation that the mean free path (mfp) at the peaks of the four lines is approximately the same at moderate temperatures.

The emitted resonance radiation is absorbed with a mfp of the order of 0.1 cm at liquid-nitrogen temperature. After the absorption, fast relaxation transitions between the four sublevels destroy phase, frequency, or angular correlations between the absorbed and re-emitted quanta. Hence, the re-emitted lines following the absorption of quanta at any particular frequency have the same profile as those produced in the surface source by the pumping radiation. The elementary profiles of individual lines cannot be directly observed. We shall assume in the following that they are either all Lorentzian

$$g_L(\nu)=1/[1+(\nu-\nu_0)^2/(\tfrac{1}{2}\Gamma)^2] \tag{1a}$$

or all Gaussian

$$g_G(\nu)=\exp[-(\nu-\nu_0)^2/(\tfrac{1}{2}\Gamma)^2]\,. \tag{1b}$$

Henceforth $g_L(\nu)$ or $g_G(\nu)$ will be referred to as "elementary profile."

On the basis of detailed balance we shall also assume that the profiles of absorption and emission lines are the same. We write for the (macroscopic) absorption cross section

$$\sigma(\nu)=\sum_{i=1}^{i=4}\sigma_{0i}g_i(\nu)\,. \tag{2}$$

As stated above the mfp $1/\sigma_{0i}$ of the four resonance lines are roughly equal. Thus, in the following analysis we shall use

$$\sigma_{0i}=\sigma_0.$$

Let us denote by q the probability that an ion in the $^6P_{7/2}$ state decays radiatively to the ground state; thus, q is the quantum yield for resonance fluorescence. It was stated above that q is nearly unity; only a few percent of the excited ions decay by vibronic or nonradiative transitions.

The probability $\tau(\nu)d\nu$ for radiative decay into the frequency range ν to $\nu+d\nu$ may now be written

$$\tau(\nu)=q\Big[\sum_{i=1}^{4}[\exp(-\Delta_i/kT)]\sigma_{0i}g_i(\nu)\Big/\times\int g_i(\nu')d\nu'\Big]\Big/[\sum_{1}^{4}\sigma_{0i}\exp(-\Delta_i/kT)], \quad (3)$$

where Δ_i is the height of the ith sublevel and T the lattice temperature.

V. THE MATHEMATICAL FORMULATION OF PHOTON TRANSPORT IN THE CRYSTAL

The physical picture of absorption and emission discussed above allows a rather simple mathematical formulation of the transport of photons in the crystal. The conservation equation for the photon flux (Boltzmann equation) may be written as follows[13]:

$$\begin{aligned}&\frac{1}{c}\frac{\partial\psi}{\partial t}+\Omega\,\mathrm{grad}\psi+\sigma(\nu)\psi=\frac{1}{4\pi}\Lambda\tau(\nu)[\phi(\mathbf{x},t)+\phi_{\mathrm{ex}}(\mathbf{x},t)]\\&\phi(x,t)=\int_{-\infty}^{t}dt'\exp[-\Lambda(t-t')]\\&\qquad\times\int d\nu'\sigma(\nu')\oint\psi(\nu',\Omega',\mathbf{x},t')d\Omega'.\end{aligned}\quad (4)$$

$\psi(\nu,\Omega,\mathbf{x},t)d\nu d\Omega d^3x$ is the photon flux at time t, in volume element d^3x, solid angle $d\Omega$, and frequency range $d\nu$. $\phi_{\mathrm{ex}}(\mathbf{x},t)$ is the density of excited atoms produced by the pumping radiation, and $\phi(\mathbf{x},t)$ is the density produced by reabsorption of resonant radiation.

Boltzmann's equation can easily be transformed into an integral equation[14] for the density of excited ions $\phi(\mathbf{x},t)$,

$$(1/\Lambda)(\partial\phi/\partial t)+\phi(\mathbf{x},t)=\int K(\mathbf{x},\mathbf{x}')[\phi(\mathbf{x}',t)+\phi_{\mathrm{ex}}(\mathbf{x}',t)]d^3x', \quad (5)$$

with the kernel[15]

$$K(\mathbf{x},\mathbf{x}')=(1/4\pi|\mathbf{x}-\mathbf{x}'|^2)\times\int d\nu\sigma(\nu)\tau(\nu)\exp[-\sigma(\nu)|\mathbf{x}-\mathbf{x}'|].$$

This integral equation can also be constructed directly by simple physical reasoning. The rate of growth of the density of excited ions $\partial\phi/\partial t$ plus the rate of decay $\Lambda\phi$ is equal to the rate of excitation. The kernel $K(\mathbf{x},\mathbf{x}')$ expresses the probability per unit time that an excited ion at $\mathbf{x}'$ decays radiatively and its excitation is transferred to an ion lying in an unit volume element at location $\mathbf{x}$.

The flux ψ in any given direction Ω and frequency ν may be obtained from ϕ by the integral

$$\psi(\nu,\Omega,\mathbf{x},t)=(\Lambda\tau(\nu)/4\pi)\times\int(\phi+\phi_{\mathrm{ex}})\exp[-s\sigma(\nu)]ds, \quad (6)$$

the integration being carried out along a ray in the direction $-\Omega$. Each of the two expressions (2) and (3) for $\sigma(\nu)$ and $\tau(\nu)$ contains a sum of four terms, corresponding to the four coupled lines omitted from the $^6P_{7/2}$ sublevels. Yet, Eq. (5), in the case under discussion, is approximately the same as if there were only a single resonance line. The kernel $K(\mathbf{x},\mathbf{x}')$ in Eq. (5) is unchanged if instead of a number of coupled lines, a single line is considered. This holds provided that the following conditions are satisfied: (1) The lines have elementary profiles with indentical functional dependence on the arguments $(\nu-\nu_{0i})/\Gamma_i$. (2) The maximum absorption cross section σ_{0i} for all coupled lines is the same. (3) The line centers are well separated so that overlap between different lines may be ignored. On the other hand, the widths of the coupled lines and the Boltzmann factors $\exp(-\Delta_i/kT)$ appearing in expression (3) for $\tau(\nu)$ may be arbitrary. The above conditions are well satisfied in the present case.

Assuming a planar geometry with a surface source at $x=0$, the Boltzmann equation for a single line with profile $g(\nu)$ is[16]

$$\begin{aligned}&\mu(\partial\psi/\partial x)+\sigma_0 g(\nu)\psi=q\Lambda g(\nu)\\&\qquad\times[\phi(x,t)+\delta(x)\phi_{\mathrm{ex}}(t)]\Big/\Big(4\pi\int g(\nu')d\nu'\Big)\\&\phi(x,t)=2\pi\sigma_0\int d\nu' g(\nu')\int_{-1}^{+1}d\mu'\\&\qquad\times\int_{-\infty}^{t}dt'\psi(\nu',\mu',x,t')\exp[-\Lambda(t-t')].\end{aligned}\quad (7)$$

This equation is to be solved with the boundary conditions

$$\psi(\nu,\mu>0,x=0,t)=0\quad\psi(\nu,\mu<0,x=L,t)=0. \quad (8)$$

[13] B. Davison and J. B. Sykes, *Neutron Transport Theory* (Oxford University Press, New York, 1957), pp. 15–22.

[14] See Ref. 13, pp. 22–27.

[15] On the right-hand side of Eq. (5) should appear the retarded time $t-(1/c)|\mathbf{x}-\mathbf{x}'|$, but as the change in ϕ is negligible in a time needed for a photon to traverse the crystal this retardation may be ignored.

[16] A term $(1/c)\partial\psi/\partial t$ on the left-hand side of Eq. (7) is omitted on the same grounds that retardation is ignored on the right-hand side of Eq. (5).

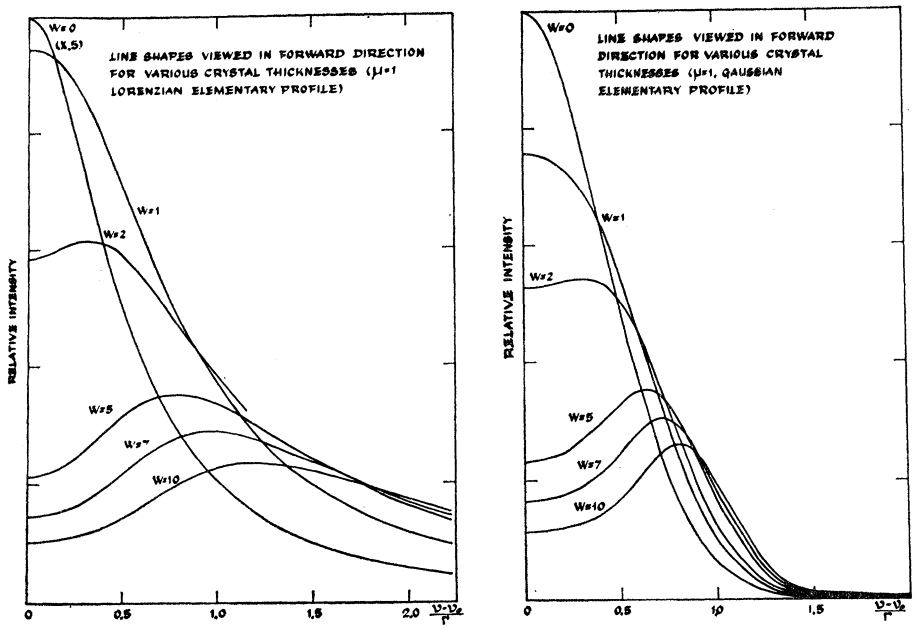

FIG. 4. Calculated line shapes of resonance radiation emanating in the normal direction to the crystal for various crystal thicknesses. (a) Lines with Lorentzian elementary profile. (b) Lines with Gaussian elementary profile.

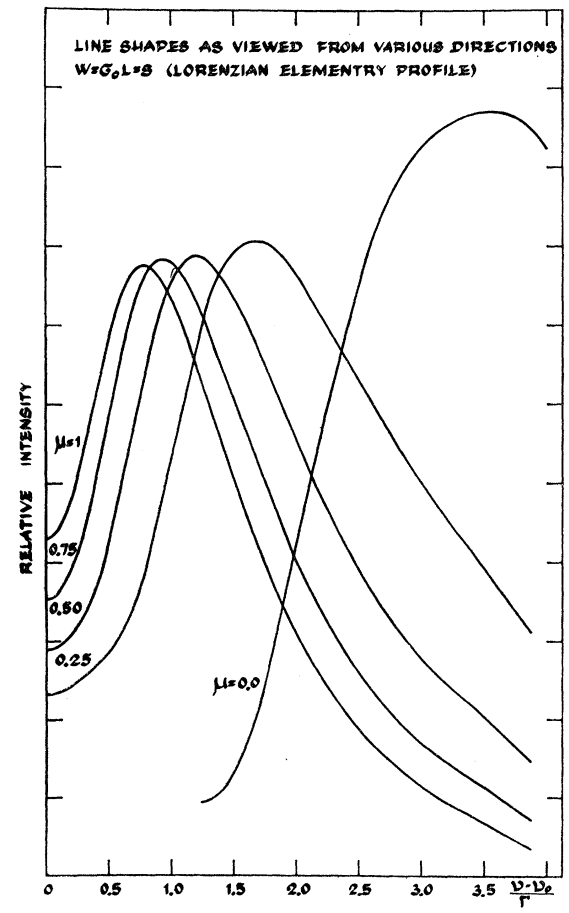

FIG. 5. Calculated line shapes of resonance radiation emanating at various directions. The crystal thickness is 5 mfp. The elementary line profile is Lorentzian.

The solutions of Eq. (7) for a given elementary profile $g(\nu)$ depend essentially on two parameters, the quantum yield q and the optical thickness $W=\sigma_0 L$ of the slab. The decay rate appears only as a scale factor for the time.

Two cases susceptible to experimental check are of interest:

(A) Continuous Excitation. In this case ϕ_{ex} and hence also the flux ψ are time independent. The line shape of radiation eminating from the crystal at the surface $X=L$ depends strongly on the direction of observation $\theta(=\arccos\mu)$ and on the optical thickness W of the crystal. In Fig. 4, line shapes are shown emitted in the normal direction to the crystal surface ($\mu=1$) for various values of W. It is seen that for thick enough crystals ($W>1$) the line is self-reversed. For very thick crystals the line becomes flattened and the double hump is hardly observed. The dependence of the line shape on the direction of observation is shown in Fig. 5. The density of excitation as a function of location and crystal thickness is given in Fig. 6.

The formation of the double hump may be understood most easily by considering the integral expression (6) for the flux. There it is immediately observed that the intensity of radiation at the center of the line is reduced by the factor $\exp(-s\sigma(\nu))$. The radiation, far in the wings of the line or nonresonant radiation terminating in unpopulated states, is proportional to the total number of ions in the excited $^6P_{7/2}$ states. The nonresonant radiation is thus enhanced by a factor

$$A=\int[\phi(x)+\phi_{ex}(x)]d^3x\Big/\int\phi_{ex}(x)d^3x,$$

compared with the case without self-trapping. In Fig. 7, the amplification factor A of nonresonant radiation is presented as function of crystal thickness (assuming a quantum yield $q=1$).

By measuring the distance between the peaks $\Delta\nu$ of the self-reversed line as a function of crystal thickness L, the mean free path (mfp), the linewidth, and to some extent the elementary profile may be determined. In Fig. 8, the logarithm of the calculated separation between the peaks $\Delta\nu/\Gamma$ is plotted against the logarithm of the optical thickness W. In order to determine experimentally the mfp σ_0^{-1} and the linewidth Γ a ln-ln plot of the experimental separation of the peaks as a function of the crystal thickness is shifted until it fits onto one of the theoretical lines of Fig. 8. One reads off the values of $\sigma_0 L$ and $\Delta\nu/\Gamma$ from the theoretical graph, thus determining σ_0 and Γ.

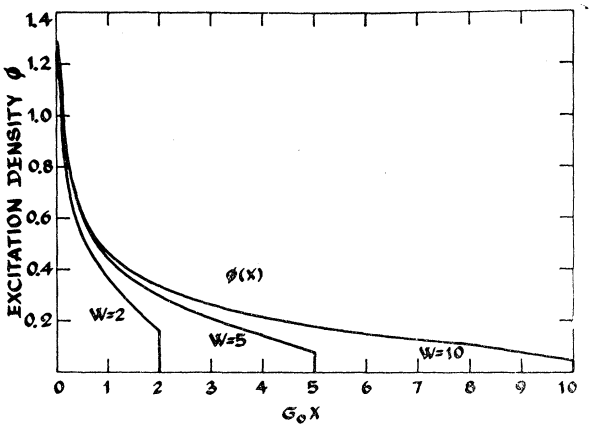

FIG. 6. Density of excited atoms as a function of location in the crystal for crystals of thickness 2, 5, and 10 mfp.

(B) Pulsed Excitation. Following a pulse of pumping radiation the photon flux decays. The decaying flux may be described by a discrete sum of exponentials[17] the amplitudes of which depend on the position and direction of observation and on the mode of excitation. After some time only the mode of longest period persists; the period: of the other modes are considerably shorter.[18] Again, measuring the decay rate λ of the fundamental mode as a function of crystal thickness L yields information on the mfp, the elementary decay rate (Λ), the quantum yield q, and the elementary line profile $g(\nu)$.

Assuming the flux to decay with a single period we insert $\psi(\nu,\mu,x,t)=\psi(\nu,\mu,x)\exp(-\lambda t)$ into Eq. (7),

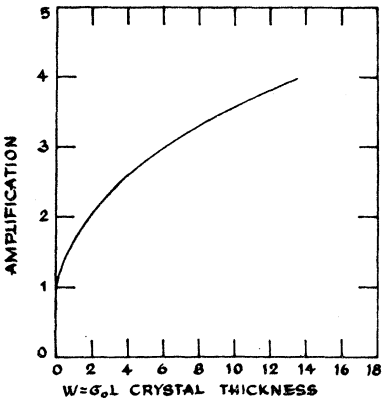

FIG. 7. Amplification factor of nonresonant radiation accompanying the resonance radiation. It is assumed that the nonresonant transition is very weak compared to the resonant transition.

obtaining

$$\mu(\partial\psi/\partial x)+\sigma_0 g(\nu)\psi=(q/4\pi)[\Lambda/(\Lambda-\lambda)]\times\left[g(\nu)\Big/\int g(\nu')d\nu'\right]\phi(x) \tag{9}$$

$$\phi(x)=2\pi\sigma_0\times\int d\nu' g(\nu')\int_{-1}^{+1} d\mu'\psi(\nu',\mu',x)\,.$$

This equation with the boundary conditions (8) poses a homogeneous problem with an eigenvalue $\gamma=(\Lambda-\lambda)/q\Lambda$, or

$$\lambda/\Lambda=1-q\gamma. \tag{10}$$

For a given elementary profile $g(\nu)$ the eigenvalues γ depend only on the optical thickness of the crystal. The longest decay period λ^{-1} corresponds to the highest eigenvalue γ_0; shorter periods correspond to lower γ's. In typical cases, the ratio between the highest eigenvalue γ_0 and the next eigenvalue γ_1 is usually of the order of 2. Yet, Eq. (10) shows that the second mode

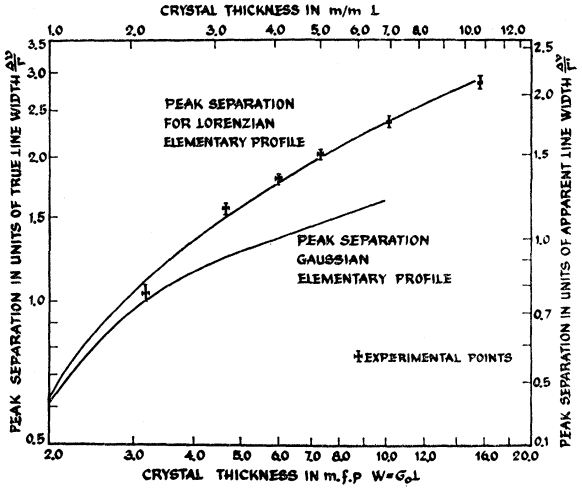

FIG. 8. Peak separation of self-reversed lines as a function of crystal thickness. The lines are observed in the normal direction to the crystal surface.

[17] See Ref. 13, p. 30.

[18] This holds only in the case that the longest period λ^{-1} is considerably longer than the decay period Λ^{-1} of an "isolated" ion.

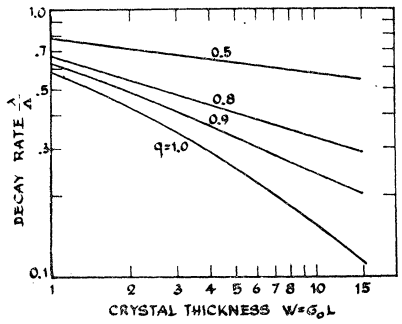

FIG. 9. Ratio of the decay constant of the fundamental mode of resonance radiation in a crystal to the decay constant of an individual atom as a function of crystal thickness W (measured in mfp's.

decays considerably faster than the fundamental mode, provided that $q\gamma_0$ is close to unity, i.e., we must have $\lambda/\Lambda \ll 1$.

To obtain σ_0, Λ and q we use a ln-ln plot of the experimentally measured decay rate λ as function of the crystal thickness L in a manner similar to that discussed in conjunction with the case of continuous excitation. The plot of experimental results is shifted until it fits into one of the lines of Fig. 9, whence the values of q, $\sigma_0 L$ and λ/Λ may be read off.

VI. ANALYSIS OF EXPERIMENTAL RESULTS

Decay rates of the resonance radiation and enhancement of the vibronics have been only qualitatively investigated.

Careful tracings were made of line shapes to determine the elementary profile, the mean free path, and linewidths. The tracings were taken mostly at liquid-nitrogen temperature at which the linewidths are of the order of the instrumental resolution. Under these circumstances, the results on thick crystals with lines broadened by self reversal yield line shapes that are in reasonable agreement with theoretical predictions (Fig. 10). On the other hand, the separation between the peaks of the self-reversed lines was found to be independent of the instrumental band pass. Consequently, the dependence of this separation on the crystal thickness was used to determine the elementary profile of the line.

The half-width Γ' of lines reflected from a crystalline powder served as a unit of frequency. Γ' is larger than the true linewidth Γ of the elementary profile because of the finite instrumental resolution and a slight self-trapping. Hence, the peak separation, measured in units of Γ' is smaller than when measured in terms of the true linewidth Γ.

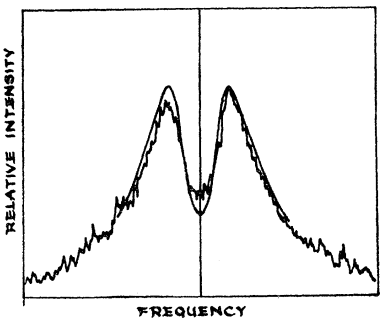

FIG. 10. Comparison of calculated to observed line shape for a crystal 10.85 mm thick.

In Fig. 8, the peak separation of the line emitted from the lowest $^6P_{7/2}$ sublevel is plotted against the crystal thickness. On this ln-ln plot the experimental results for the peak separation are shown as points. The peak separation $\Delta\nu$ is measured in units of Γ' (upper scale of the diagram) and the crystal thickness L is measured in millimeters (right-hand scale of the diagram). Theoretical curves for $\Delta\nu/\Gamma$ as a function of $\sigma_0 L$ are drawn for Lorentzian and Gaussian elementary profiles. The experimental results fit the theoretical curve for a Lorentzian profile if the two scales are shifted so that $\Delta\nu/\Gamma = 1.35\Delta\nu/\Gamma'$ and $L = 0.68$ mm corresponds to $\sigma_0 L = 1$. This means that the mfp is about 0.68 mm and the true linewidth Γ is narrower by a factor of 1.35 than the apparent width determined by reflection from powder.

The experimental points can also be fitted to a curve based on a Gaussian profile. However, this can be done only if the experimental scale $\Delta\nu/\Gamma'$ is shifted below the theoretical scale $\Delta\nu/\Gamma$ so that $\Gamma > \Gamma'$. This result should be rejected since the observed width can only be larger than the true width.

TABLE I. Linewidths and mean free paths for the four gadolinium emission lines at 77°K.

Line No.	Γ' cm^{-1}	Γ'/Γ	Γ cm^{-1}	σ_0^{-1} mm
1	1.30	$1.35_{-0.07}^{+0.15}$	$0.96_{-0.09}^{+0.05}$	$0.68_{-0.13}^{+0.08}$
2	1.58	$1.60_{-0.18}^{+0.20}$	$0.99_{-0.11}^{+0.12}$	$0.56_{-0.12}^{+0.13}$
3	1.92	$1.38_{-0.18}^{+0.22}$	$1.39_{-0.19}^{+0.21}$	$0.58_{-0.13}^{+0.14}$
4	1.65	$1.25_{-0.15}^{+0.25}$	$1.32_{-0.22}^{+0.18}$	$0.65_{-0.18}^{+0.16}$

The results of fitting the four $^6P_{7/2} \rightarrow {}^8S_{7/2}$ transitions at liquid-nitrogen temperatures to Lorentzian profiles are compiled in Table I. The experimental results can be brought to fit the theoretical predictions within the indicated limits. The mfp for the four transitions is found to be the same within the experimental accuracy. The linewidth tends to grow for the higher levels as expected for lifetime broadening.[11] At lower temperatures, the intensity of emission from the upper sublevels decreases, and the line emitted from the lowest sublevel becomes sharper. No quantitative measurements were made at temperatures lower than liquid nitrogen since the instrumental band-pass could not be reduced enough.

VIII. DISCUSSION

The preceding results show that self-reversal can be used to obtain the elementary profiles and linewidths of resonance transitions in crystals. To a certain limit this can be done even when direct tracing of the line

profile is difficult because of the large instrumental band pass.

The elementary profile of the resonance transitions in gadolinium chloride was found to be Lorentzian. This corresponds to lifetime broadening due to relaxation between the emitting sublevels. It is interesting to speculate about the change of the linewidth when the temperature is reduced below that of liquid nitrogen. Let Δ denote the energy separation between the lowest two sublevels of $^6P_{7/2}$ and let the temperature be low enough to satisfy the relation $kT<\Delta$. We assume further that the width of the line emitted from the lowest sublevel is determined by the relaxation rate $R\exp(-\Delta/kT)$ to the next higher level. Here R is a constant representing the probability for spontaneous emission of phonons from the second to the lowest $^6P_{7/2}$ sublevel. Due to the strong temperature-dependent factor $\exp(-\Delta/kT)$, the relaxation becomes very small at liquid-helium temperature. It is estimated to be a few parts of hundred thousands of a wave number. When the relaxation broadening becomes so small other mechanisms may determine the actual linewidth. Among these, an important factor is due to self-trapping. As the elementary profile narrows, the mean free path is reduced, and the apparent width is determined by the finite photon lifetime in the crystal. It is difficult to account for this broadening at such temperatures. Strain broadening, expected to be small in crystals grown from solutions, may, nevertheless, contribute to the width at 4°K. Further investigations are needed to determine the low-temperature behavior of linewidths in these crystals.

PHYSICAL REVIEW VOLUME 137, NUMBER 5A 1 MARCH 1965

Flux Methods for the Analysis of Transport Problems in Semiconductors in the Presence of Electric Fields*

J. P. McKelvey and J. C. Balogh†
Department of Physics, The Pennsylvania State University, University Park, Pennsylvania
(Received 7 October 1964)

A calculational technique based upon the detailed study of flux interactions between various parts of a diffusion-recombination system, whose foundations have been discussed elsewhere in the literature, is extended to include cases where electric fields may be acting upon the particles of the system. The analysis is worked out in detail for systems obeying Boltzmann statistics in which the field satisfies the condition $\mu E_0 << \bar{c}$, where $\bar{c}$ is the mean thermal velocity. Analytic solutions for the reflection and transmission coefficients of a sheet of material of arbitrary thickness for incident carriers are worked out for constant electric fields; approximate or numerical methods are applicable for nonconstant fields. The effect of the details of scattering and recombination processes upon the solutions is considered. A simple example is worked out to exhibit areas of agreement between this method and the more conventional calculational techniques and to demonstrate certain advantages in generality and conceptual simplicity associated with the flux method.

I. INTRODUCTION

A FEW years ago, an alternative calculational technique for the solution of diffusion-recombination transport problems was proposed and discussed in detail in an article[1] which will be referred to hereafter as (I). The immediate application of this method, which we shall call the *flux method*, was to the solution of added carrier transport problems in semiconductors, although of course the range of potential applications is much broader. In a second article[2] [designated hereafter by (II)], the technique was developed into a rational scheme of analysis for one-dimensional semiconductor *p-n* junctions and junction devices in the steady state. The flux technique, although inherently limited to one-dimensional steady-state systems, possesses certain advantages over the conventional calculational technique of solving the diffusion equation under appropriate boundary conditions. The most important of these advantages are (i) conceptual simplicity and an enhanced physical insight into the interaction between bulk and surface regions and between scattering and absorptive processes, (ii) the ease and precision with which boundary conditions at surfaces and internal boundaries (such as *p-n* junctions, grain boundaries, or dislocation sheets) may be introduced, (iii) the fact that the influence of the absorption free path upon the effective diffusion coefficient (and thus the dependence of the effective diffusion coefficient upon *both* scattering and absorption free paths) is incorporated into the theory from the outset, and (iv) that the flux method, unlike the simplest form of the diffusion theory, is directly applicable to systems whose physical

* Work supported in part by U. S. Air Force Office of Scientific Research.
† Present address: Department of Physics, U. S. Air Force Academy, Colorado.
[1] J. P. McKelvey, R. L. Longini, and T. P. Brody, Phys. Rev. **123**, 51 (1961).
[2] J. P. McKelvey, J. Appl. Phys. **33**, 985 (1962).

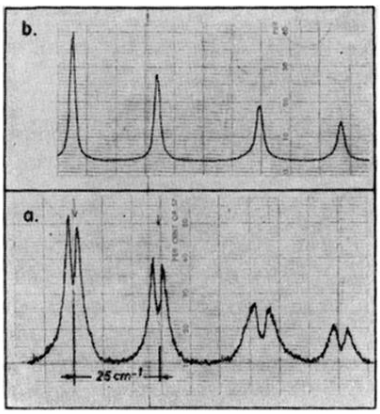

FIG. 3. Resonance fluoresence in $GdCl_3 \cdot 6H_2O$ at 77°K. (a) Shape of lines observed in the forward direction. (b) Shape of the same lines observed in the backward direction.